JACS
JOURNAL OF THE AMERICAN CHEMICAL SOCIETY
Article
pubs.acs.org/JACS

Base-Catalyzed Aryl-B(OH)$_2$ Protodeboronation Revisited: From Concerted Proton Transfer to Liberation of a Transient Aryl Anion

Paul A. Cox,[†,⊥] Marc Reid,[†,⊥] Andrew G. Leach,[‡] Andrew D. Campbell,[§] Edward J. King,[∥] and Guy C. Lloyd-Jones*[,†]

[†]School of Chemistry, University of Edinburgh, Joseph Black Building, David Brewster Road, Edinburgh EH9 3FJ, U.K.
[‡]School of Pharmacy and Biomolecular Sciences, Liverpool John Moores University, Byrom Street, Liverpool L3 3AF, U.K.
[§]AstraZeneca, Silk Road Business Park, Macclesfield SK10 2NA, U.K.
[∥]TgK Scientific Limited, 7 Long's Yard, St Margaret's Street, Bradford-on-Avon BA15 1DH, U.K.

Supporting Information

ABSTRACT: Pioneering studies by Kuivila, published more than 50 years ago, suggested ipso protonation of the boronate as the mechanism for base-catalyzed protodeboronation of arylboronic acids. However, the study was limited to UV spectrophotometric analysis under acidic conditions, and the aqueous association constants (K_a) were estimated. By means of NMR, stopped-flow IR, and quenched-flow techniques, the kinetics of base-catalyzed protodeboronation of 30 different arylboronic acids has now been determined at pH > 13 in aqueous dioxane at 70 °C. Included in the study are all 20 isomers of $C_6H_nF_{(5-n)}B(OH)_2$ with half-lives spanning 9 orders of magnitude: <3 ms to 6.5 months. In combination with pH−rate profiles, pK_a and $\Delta S^{\ddagger}$ values, kinetic isotope effects (^{2}H, ^{10}B, ^{13}C), linear free-energy relationships, and density functional theory calculations, we have identified a mechanistic regime involving unimolecular heterolysis of the boronate competing with concerted ipso protonation/C−B cleavage. The relative Lewis acidities of arylboronic acids do not correlate with their protodeboronation rates, especially when ortho substituents are present. Notably, 3,5-dinitrophenylboronic acid is orders of magnitude more stable than tetra- and pentafluorophenylboronic acids but has a similar pK_a.

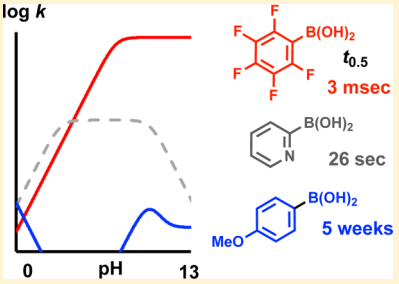

INTRODUCTION

Boronic acids have a long history of application in the chemical sciences.[1] They provide conveniently handled or in situ-generated[2] nucleophiles for a host of cross-coupling and substitution reactions.[3] However, their application extends far wider than this, as they have found use, for example, as radical precursors,[4] as Lewis acid catalysts,[5] in aryl deuteration,[6] as traceless catalyst-directing groups,[7] as chemosensors,[8] as functional groups in materials,[9] as gelators,[10] as self-healing polymers,[11] in ^{18}F labeling,[12] and in drug design.[13]

An understanding of the factors that control the stability of boronic acids can inform their more effective application. One of the primary decomposition pathways of arylboronic acids is protodeboronation,[14] the conversion of Ar−B(OH)$_2$ to Ar−H. The process is generally an undesired one, reducing yields and increasing the amounts of side products.[15] In some circumstances, however, protodeboronation is productive.[16] This includes, for example, the traceless removal of a B(OH)$_2$ blocking[16a] or directing group,[16b] in deborylative synthetic strategies,[16c] or for the in situ purging of genotoxic[17] arylboronic acid residues from Suzuki−Miyaura reactions. As a consequence, the acceleration of protodeboronation is a field of significant current interest.[18]

Mechanistic insight into the impact of aqueous base and acid on the rate of protodeboronation is particularly useful in the context of Suzuki−Miyaura cross-coupling.[3a,b] For basic heteroarylboronic acids, the effects can be complex and counterintuitive.[14m] In contrast, nonbasic heteroaryl-, alkyl-, and vinylboronic acids undergo simple acid- and base-catalyzed processes.[14m] In seminal early studies, Kuivila[14c−e] measured the rates of aqueous acidic protodeboronation (90 °C, pH range 2.0 to 6.7; UV−vis spectrophotometry) of a small series of monosubstituted arylboronic acids.[14e] Kuivila deduced from these data that in addition to an acid-catalyzed pathway involving the boronic acid, there is a mechanism involving the boronate ([ArB(OH)$_3$]$^-$) generated in a pH-controlled equilibrium (K_a).[19] The rates of protodeboronation could not be determined above pH 7 because of the appearance of strongly UV-absorbing side products.[14e] Nonetheless, the limiting reaction rates estimated by extrapolation to pH > 13 ($k_{rel(est.)}$; Scheme 1)[20] appeared to show that protodeboronation is retarded by a fluorine substituent at the meta position and accelerated by a fluorine at the ortho or para position. The greater acceleration by *o*-F was ascribed to electrostatic repulsion between B(OH)$_3^-$ and F.

However, the effects of fluorine substituents are dichotomous. Compare for example, phenyl-, 4-fluorophenyl-, and 3-

Received: July 17, 2017
Published: August 21, 2017

ACS Publications © 2017 American Chemical Society

DOI: 10.1021/jacs.7b07444
J. Am. Chem. Soc. 2017, 139, 13156−13165

fluorophenylboronates, which have nearly identical rates ($k_{rel(obs)}$; Scheme 1) whereas in the analogous *o*-fluorinated series (2-fluorophenyl, 2,4-difluorophenyl, and 2,5-difluorophenyl), the 4-F and 3-F substituents induce significant rate acceleration. The origins of these effects are the subject of the work presented herein.

Scheme 1. Dichotomous Effects of F Substituents on the Relative Rates[20] of Aqueous Protodeboronation of Arylboronates

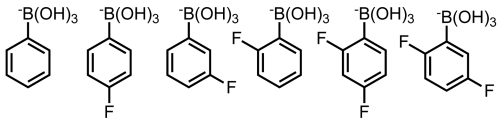

$k_{rel\ (est.)}$	1.0	1.4	0.3	11	--	--	*Kuivila*
$k_{rel\ (obs)}$	1.0	1.4	0.98	243	616	1548	*This work*

We report kinetic data for the base-catalyzed protodeboronation of 30 arylboronic acids, including all isomers of $C_6H_nF_{(5-n)}B(OH)_2$ (n = 0 to 5). Some of these species are many orders of magnitude more reactive than the notoriously unstable[21] 2-pyridyl system (half-life ($t_{0.5}$) = 27 s at 70 °C, pH 7 in 50% aqueous dioxane).[14m] In combination with thermodynamic reaction parameters, pH–rate profiles, pK_a determinations, computational analysis, the effect of the countercation ($[ArB(OH)_3]^-[M]^+$), kinetic isotope effects (KIEs) (^{2}H, ^{10}B, ^{13}C), and linear free-energy relationships (LFERs), a dual mechanistic regime is identified for arylboronic acid protodeboronation. The study shows that trihydroxyborates generated from highly electron-deficient arylboronic acids under aqueous conditions are inherently unstable. Highly electron-deficient arylboronic acids have negligible susceptibility to acid-catalyzed protodeboronation, and their Lewis acidity is not directly related to their rates of protodeboronation under basic conditions.

RESULTS AND DISCUSSION

Electron-deficient and ortho-substituted arylboronic acids have considerable utility in cross-coupling,[14i,22] as catalysts,[5] and in sensors.[8] Some of these species undergo rapid decomposition under basic conditions. For example, polyfluorophenylboronic acids require specialized catalysts to be efficiently cross-coupled.[14i,22] Data on the base-mediated protodeboronation of various classes of electron-deficient arylboronic acids and boronates are available from prior studies by Kuivila,[14e] Fröhn,[14g] Cammidge,[14h] Buchwald,[14i] Perrin,[14j] and Adonin.[14k] However, a holistic mechanistic analysis is limited by (i) the restricted range of substrates for which comparable kinetic data have been reported, (ii) the wide variations in conditions employed among studies, and (iii) an absence of pH–rate profiling and pK_a data in the majority of cases. Nonetheless, the above studies[14e,g–k] reveal that all 2,6-dihalogenated phenylboronic acids are highly susceptible to protodeboronation when exposed to base.

1. Acquisition of the Kinetic Data Set. In order to study the mechanism of protodeboronation of electron-deficient arylboronic acids in more detail, we selected 30 examples (**1**–**30**; Table 1) for kinetic analysis. The selection deliberately includes a number of examples that overlap with previous studies.[14e,h–j] Obtaining a coherent set of kinetic data across the whole series required careful choice of reaction conditions and methodology. A 1:1 mixture of H_2O and dioxane at 70 °C (26.8 M H_2O; see the Supporting Information (SI)) was found to give tractable boronic acid solubility across a wide range of pH and salt concentrations. These conditions also allow direct comparison of kinetic data for **1**–**30** with those for 16 heteroaromatic boronic acids, including the highly reactive 2-pyridyl and 5-thiazolyl species.[14m]

Table 1. Aqueous Association (pK_a) and Protodeboronation (k_{PDB}; M = K) of Arylboronates 1–30$_{OH}$ at 70 °C in 1:1 H_2O/Dioxane

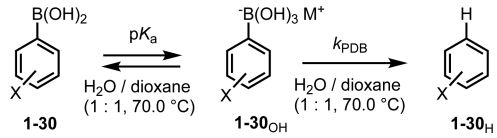

1-30 **1-30$_{OH}$** **1-30$_H$**

substrate; X	pK_a	log k_{PDB}	~$t_{0.5}$
1; 3-F	10.46[a]	−7.40	7 months
2; H	11.25[a]	−7.39	6 months
3; 4-F	10.97[a]	−7.23	4 months
4; 3,4-F_2	10.34[a]	−7.13	3 months
5; 3,5-F_2	9.78[a]	−7.08	3 months
6; 3-Cl	10.56[a]	−6.85	8 weeks
7; 3,5-$(CF_3)_2$	9.38[a]	−6.81	7 weeks
8; 4-Me	11.75[a]	−6.80	7 weeks
9; 3,4,5-F_3	9.44[a]	−6.77	7 weeks
10; 4-MeO	11.78[a]	−6.62	5 weeks
11; 3,5-$(NO_2)_2$	7.91[a]	−4.92	16 h
12; 2-F-4-MeO	10.78[a]	−5.25	34 h
13; 2-F	10.14[a]	−5.00	19 h
14; 2,4-F_2	10.02[a]	−4.60	8 h
15; 2,5-F_2	9.34[a]	−4.20	3 h
16; 2-F-4-CF_3	9.04[a]	−4.03	2 h
17; 2,3-F_2	9.51[a]	−3.92	2 h
18; 2,4,5-F_3	9.00[a]	−3.76	1 h
19; 2,3,4-F_3	9.06[a]	−3.53	39 min
20; 2-F-5-NO_2	8.22[b]	−3.10	15 min
21; 2,3,5-F_3	8.47[a]	−2.95	10 min
22; 2,3,4,5-F_4	8.91[b]	−2.41	3 min
23; 2,6-F_2-4-MeO	9.56[b]	−1.01	7 s
24; 2,6-F_2	9.15[b]	−0.87	5 s
25; 2,4,6-F_3	9.03[b]	−0.26	1 s
26; 2,3,6-F_3	8.66[b]	0.47	235 ms
27; 2,3,4,6-F_4	8.39[b]	1.02	66 ms
28; 2,3,5,6-F_4	7.97[b]	1.79	11 ms
29; 2,3,5,6-F_4-4-MeO	8.33[b]	1.88	9 ms
30; 2,3,4,5,6-F_5	7.67[b]	2.43	2.6 ms

[a]Measured by ^{11}B NMR pH titration. [b]Estimated by correlation of the pH dependence of the protodeboronation rate using $k_{obs(OH)} = k_{PDB}/\{1 + 10^{(pK_a - pH)}\}$ (see the SI).

Protodeboronation reactions of **1**–**30** were conducted at pH ≥ 13 (vide infra). Under these conditions, the reactant is exclusively in its boronate form, and the resulting (pseudo) first-order decays (k_{obs}/s^{-1}) are pH-independent, without complication from self- or autocatalysis.[14m] Reactions were initiated by addition of a solution of strong base (excess KOH) to a solution of the boronic acid and quenched, if required, by pH drop (excess HCl). Automated flow techniques were employed for fast reactions, allowing thermostated rapid mixing of the various solutions. Aqueous dioxane stock solutions of the boronic acids contained 10 mol % propionic or trifluoroacetic acid as combined internal NMR reference and stabilizer. The most reactive (**27**–**30**) required 110 mol % trifluoroacetic acid

DOI: 10.1021/jacs.7b07444
J. Am. Chem. Soc. 2017, 139, 13156–13165

to avoid significant protodeboronation of the stock solution prior to addition of the base at 70 °C.

The wide scale of reactivity encountered for **1**–**30** required that a range of techniques be applied for determination of the reaction kinetics. Slow reactions ($t_{0.5}$ of days to months) were conducted in sealed quartz[14m] NMR tubes at 70 °C and monitored periodically by ^{1}H or ^{19}F NMR spectroscopy at 70 °C. Reactions with intermediate rates ($t_{0.5}$ of hours) were again set up in quartz NMR tubes at 70 °C, but as a series, with manual pH quenching of individual tubes at increasing time intervals followed by analysis by ^{1}H/^{19}F NMR spectroscopy at ambient temperature. Fast reactions ($t_{0.5}$ of seconds to minutes) were analyzed in situ at 70 °C using a stopped-flow attenuated total reflectance FTIR (SF-ATR-FTIR) device. Very fast reactions ($t_{0.5}$ of milliseconds) were conducted by rapid quenched flow at 70 °C prior to off-line analysis by ^{19}F NMR spectroscopy.

2. Correlation of Kinetics with pH. In his pioneering studies on protodeboronation, Kuivila used pH extrapolation[20] to predict the Hammett correlation for reaction under strongly basic conditions, despite being unable to directly measure this. On the basis of the negative gradient found for the correlation (ρ = −2.3),[23] he proposed that protodeboronation involves ipso protonation of an arylboronate intermediate by water (pathway I in Scheme 2).[14e] Two alternative pathways (II and III) have been proposed by Fröhn[14g] and Perrin[14j] to account for the rapid protodeboronation of ortho-halogenated systems. Both mechanisms invoke an *o*-halogen-induced Brønsted acidity in the B–OH functionality, in either the boronic acid (pathway II) or the boronate (pathway III).

Scheme 2. Mechanisms I–III Previously Proposed for Base-Catalyzed Protodeboronation of Arylboronic Acids

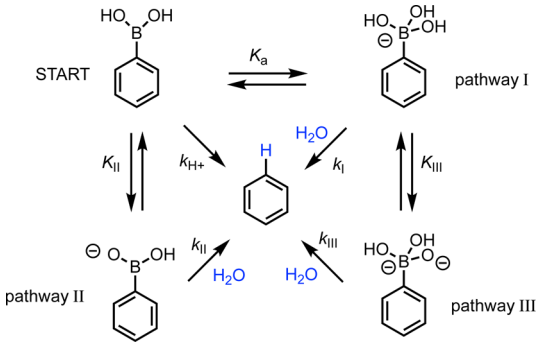

In our earlier study on heteroaromatic boronic acids, we demonstrated that a detailed pH–rate profile (pH 1–13) allows correlation of speciation, $[H]^+/[OH]^-$ concentration, and rate with changes in mechanism.[14m] Indeed, this technique allowed us to deduce that the kinetically unique Perrin mechanism[14j] (pathway III) is responsible for the rapid protodeboronation of 4-pyrazolyl- and 3,5-dimethyl-4-isoxazolylboronates under strongly basic conditions (pH ≥ pK_a + 2).[14m]

A pH–rate analysis was thus conducted for 2,6-difluorophenylboronic acid (**24**, pK_a = 9.15), one of the faster-reacting arylboronic acids in the series **1**–**30**. The rate of its protodeboronation increases >6 orders of magnitude as the buffer pH is raised from 1 to 13 (Figure 1A). Mechanisms proceeding via a monoanion, generated either by association of OH^- (pathway I) or by deprotonation of B–OH (pathway II),

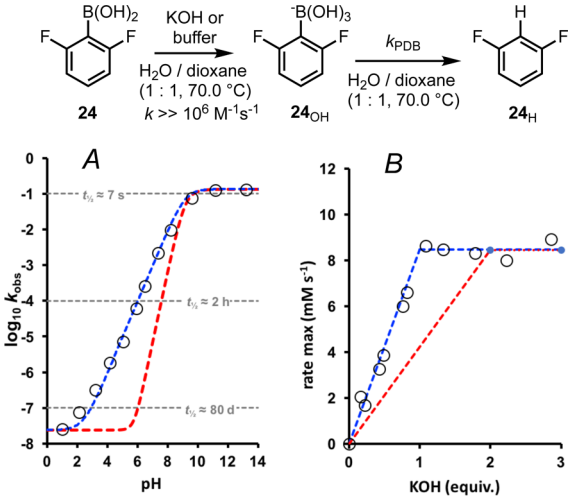

Figure 1. Protodeboronation of 2,6-difluorophenylboronic acid (**24**) (51 mM) at 70 °C. Circles represent experimental data. (A) pH–log k_{obs} profile; buffered pH. Blue line: monoanionic mechanisms (e.g., I/II/IV), where $k_{obs} = k_{PDB}/\{1 + 10^{(pK_a-pH)}\} + k_b$, with p$K_a$ = 9.15, k_{PDB} = 0.135 s^{-1}, and $k_b = 3 \times 10^{-8}$ s^{-1}. The last value corresponds to a very slow uncatalyzed process.[14e,m] Red line: mechanism III, where $k_{obs} = k'_{III}\{10^{(pH-pK_w)}\}/\{1 + 10^{(pK_a-pH)}\} + k_b$, with p$K_a$ = pK_{III}, k'_{III} = 0.135 s^{-1}, and $k_b = 3 \times 10^{-8}$ s^{-1}. (B) Dependence of the rate on the KOH stoichiometry.

are kinetically indistinguishable in terms of pH dependence: $k_{obs(OH)} = k_{PDB}/\{1 + 10^{(pK_a-pH)}\}$. For **24** (p$K_a$ = 9.15), this function predicts a linear correlation (gradient +1) of $\log_{10} k_{obs}$ versus pH at pH values below 7.15 (pK_a − 2). At pH values above this, the gradient progressively attenuates, becoming zero (i.e., the rate is pH-independent) for pH ≥ 11.15 (pK_a + 2). This simple model correlates well with the data, as can be seen from the dashed blue line in Figure 1A. There is no evidence for any significant acid catalysis ($k_{obs(H^+)} = k_H/\{10^{pH}[1 + 10^{(pH-pK_a)}]\}$) or bimolecular contributions from self/autocatalysis in the pH region close to pK_a.[24]

Mechanism III is kinetically distinct from I and II ($k_{obs} = k'_{III}\{10^{(pH-pK_w)}\}/\{1 + 10^{(pK_a-pH)}\}$)[25] even when p$K_a$ = pK_{III} (dashed red line in Figure 1A). An exception to this is if two mechanisms are operating in parallel, with $k_{PDB} = k_{III}$ *and* pK_a = pK_{III}. To test this possibility, the rate of protodeboronation[26] of **24** was determined as a function of initial [KOH]/[**24**] ratio. There is a clear "saturation" in hydroxide for [KOH]/[**24**] ≈ 1.0 (Figure 1B). Mechanisms proceeding via equilibration of the boronic acid with the monoanion (boronate) reach a rate maximum when the initial ratio is close to unity. Mechanism III, which proceeds via a formally dianionic pathway, requires superstoichiometric KOH to reach rate saturation (dashed red line). The same hydroxide dependence (dashed blue line) was observed at 21 °C. Pentafluorophenylboronic acid (**30**), the most reactive substrate in the series, behaved analogously (see the SI).

3. Dichotomous LFER. As noted above, the disparate effects of electronegative substituents (Scheme 1) were interpreted by Kuivila within the context of mechanism I: electrostatic repulsion (*o*-X) accelerates protonolysis of the boronate, whereas inductive effects (*m*/*p*-X) attenuate it.[14e] Since the electronic influences of sterically unencumbered substituents should be independent (i.e., their Hammett σ values should be additive),[27] predictable effects should arise from ortho versus meta/para multiple substitutions. This aspect

DOI: 10.1021/jacs.7b07444
J. Am. Chem. Soc. 2017, 139, 13156–13165

was tested by LFER correlation of three subgroups (separated by horizontal lines in Table 1): those with no ortho substituent (**1**–**11**, group 1), those with a single *o*-fluoro substituent (**12**–**22**, group 2), and those with two *o*-fluoro substituents (**23**–**30**, group 3).

Isolating the three subgroups means that if the same mechanism (I or II) is operative throughout, each group should show a similar correlation (ρ) to that predicted by Kuivila (ρ = −2.3) for the monosubstituted *m*/*p*-X-C_6H_4–$B(OH)_2$ series.[14e] However, as shown in Figure 2, subgroups 2 and 3 both have a positive gradient (ρ = +4), whereas subgroup 1 has a flat, marginally concave profile.

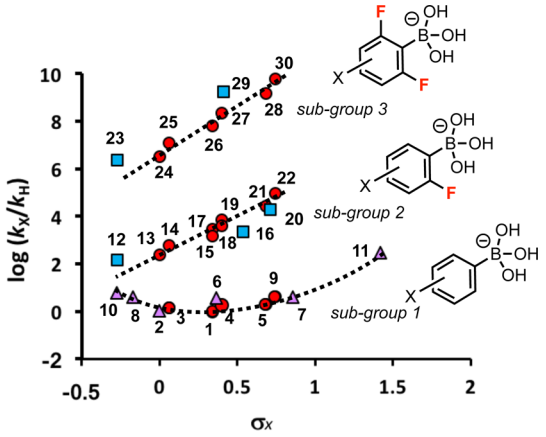

Figure 2. Hammett analyses of protodeboronation of arylboronic acids **1**–**11** (subgroup 1), **12**–**22** (subgroup 2), and **23**–**30** (subgroup 3) using 50 mM $RB(OH)_2$ in 1:1 H_2O/dioxane at 70 °C with pH > pK_a + 2. Dashed lines through data are solely guides to the eye. Red circles: substrates with fluorine substituents only. Blue squares: substrates with additional non-fluorine substituents. Purple triangles: non-fluorinated substrates.

The 3,5-dinitro-substituted boronic acid **11** (σ = 1.42) is an evident outlier in subgroup 1, undergoing protodeboronation around 2 orders of magnitude faster than **1**–**10**. The similar positive-gradient correlations in subgroups 2 and 3 show that an additional *o*-fluoro substituent accelerates the reaction by a factor of approximately 2.5 × 10^4. Further inspection of subgroups 2 and 3 shows that MeO, CF_3, and NO_2 substituents (blue squares in Figure 2) cause consistent small deviations from the trend exhibited by the *solely* fluorinated systems (red circles in Figure 2). The directions of displacement are indicative that standard σ values overestimate the resonance contribution by MeO (**12**, **23**, **29**) and underestimate the inductive effects of CF_3 (**16**) and NO_2 (**20**) for this particular mechanism.

To refine the analysis of **1**–**30**, a Swain–Lupton (SL) correlation combining all of the above observations was constructed (Figure 3). A field-dominated parametrization (0.69*F* + 0.31*R*) was applied to reduce the resonance contributions of MeO and F, and to unify the three subgroups an empirical value[28] of $\sigma^{o\text{-F}}$ = 1.24 was included for each *o*-F substituent. The resulting correlation has two regions: that with $\sigma^{SL} \geq 0.7$ is mechanistically continuous (ρ^{SL} = +3.4) and mechanistically distinct from that with $\sigma^{SL} \leq 0.7$.

The region with $\sigma^{SL} \leq 0.7$ predominantly contains substrates studied by Kuivila as part of the monosubstituted *m*/*p*-X-C_6H_4–$B(OH)_2$ series, for which mechanism I was proposed.[14e] Importantly, 3,4,5-trifluorophenylboronic acid (**9**, σ^{SL} = 0.84)

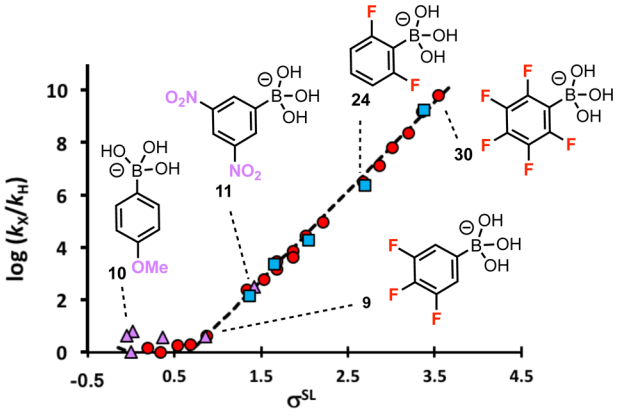

Figure 3. LFER for the protodeboronation of the boronate forms of arylboronic acids **1**–**30** using a modified Swain–Lupton parameter, σ^{SL} = 0.69*F* + 0.31*R* + *n*$\sigma^{o\text{-F}}$, where $\sigma^{o\text{-F}}$ = 1.24 and *n* is the number of *o*-F substituents. Symbol coding: see Figure 2.

and 3,5-dinitrophenylboronic acid (**11**, σ^{SL} = 1.42) lie within and upon the correlation for the upper region ($\sigma^{SL} \geq 0.7$). This indicates that it is the combined electronic effect (predominantly inductive) of the substituents that controls which of the two distinct mechanistic pathways is followed, *not* the specific presence of halogens or ortho substituents.[14j]

4. Lewis Acidity of $ArB(OH)_2$ Species. Polyfluorinated arylboronic acids have been proposed to possess enhanced Brønsted acidity (pathway II in Scheme 2), providing an alternative[14g] pathway to the Kuivila mechanism (pathway I in Scheme 2).[14e] Although these mechanisms (I and II) are kinetically indistinguishable (vide supra), trigonal/tetrahedral boron centers related by equilibrium have characteristic differences in their ^{11}B NMR chemical shifts and line widths.[29] For boronic acids in aqueous media, rapid intermolecular exchange (~10^6 M^{-1} s^{-1}) of hydroxyl ligands between boronic and boronate centers results in a single time-averaged, population-weighted ^{11}B NMR signal, with $\Delta\delta_B$(tet → trig) ≈ 30 ppm.[29] The majority of boronic acids **1**–**30** proved to be stable enough at 70 °C for $^{11}B\{^1H\}$ NMR pH titration studies. The 20 examples (**1**–**19** and **21**) that could be analyzed in detail (see the SI) span both of the mechanistic regimes identified by the Swain–Lupton analysis (above and below σ^{SL} = 0.7; Figure 3). All of the examples displayed time-averaged ^{11}B NMR chemical shifts and line widths characteristic of generation of a Lewis acid adduct, i.e., a tetrahedral boronate, $[ArB(OH)_3]^-$, for which K_a (Table 1) was determined using the Henderson–Hasselbalch relationship. Since the rate of protodeboronation (k_{obs}) directly correlates with the *boronate* population (K_a, Figure 1A), there is no evidence for any significant contribution by mechanism II under these highly aqueous conditions.[30]

Analysis of the entire data set (Table 1) shows that the impact of *o*-F substitution on the Lewis acidity of the boronic acid (K_a) is much less marked than the impact on the rate of decomposition (k_{obs}) of the corresponding boronate. The Lewis acidity can be correlated using regular Hammett σ values for meta and para substituents, again normalizing the three groups of boronic acids by inclusion of an empirical value[28] ($\sigma^{o\text{-F}}$ = 0.45) for each *o*-F substituent (Figure 4).[31] Although 1:1 H_2O/dioxane increases the pK_a of arylboronic acids by approximately 2 units relative to that measured in water,[5j,14m,29,31] the *relative* Lewis acidities are not significantly

DOI: 10.1021/jacs.7b07444
J. Am. Chem. Soc. 2017, 139, 13156–13165

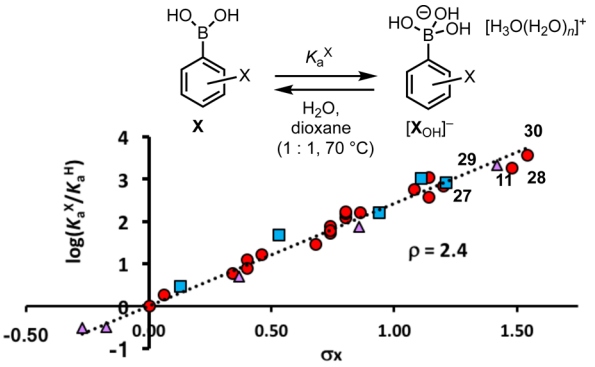

Figure 4. Modified Hammett correlation of the aqueous association constant (K_a) to generate $[ArB(OH)_3]^-[H_3O(H_2O)_n]^+$ in 1:1 H_2O/dioxane at 70 °C for arylboronic acids **1**−**30**, where $\sigma = \sigma_x + n\sigma^{o\text{-F}}$, in which $\sigma^{o\text{-F}} = 0.45$ and n is the number of *o*-F substituents. Symbol coding: see Figure 2.

changed: $\rho = 2.4$ versus $\rho = 2.1$ in H_2O at ambient temperature.[31]

5. Protodeboronation via Mechanism I. Of the 30 arylboronic acids studied, eight (**1**−**6**, **8**, and **10**) are in the $\sigma^{SL} \leq 0.7$ region of the Swain−Lupton analysis (Figure 3) and are mechanistically distinct from those with $\sigma^{SL} \geq 0.7$. Six of these (**1**−**3**, **6**, **8**, and **10**) were previously studied by Kuivila (at 90 °C in malonate-buffered water, pH 6.7), who proposed an aromatic electrophilic substitution pathway via ipso protonation of the arylboronate by H_2O (mechanism I_A in Scheme 3).[14e]

Scheme 3. Stepwise (I_A)[14e] and Concerted (I_B) Mechanisms for Base-Catalyzed Arylboronic Acid Protodeboronation

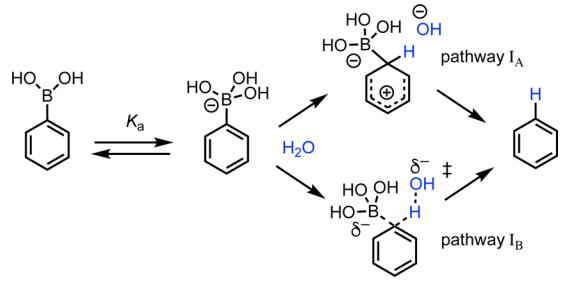

However, key in the analysis was a series of data that were determined under acidic conditions (pH 6.7, 25 °C, uncorrected) and then normalized for LFER correlation ($\rho = -2.3$) by calculation of the boronate population using estimated K_a values.[14e,19,20]

By conducting reactions at high pH, we have directly determined the rates of protodeboronation of the arylboronates. The data for boronates **1**−**3**$_{OH}$, **6**$_{OH}$, **8**$_{OH}$, and **10**$_{OH}$ ($\sigma_{SL} \leq 0.7$; Figure 3) show that the rate (k_{obs}) is less sensitive to the substituents ($|\rho| \leq 1$) than previously estimated by Kuivila.[14e] This aspect was explored computationally. A transition state (TS) could not be located (DFT, M06L/6-311++G**)[32] for a stepwise protonation mechanism (pathway I_A). Instead, the lowest-barrier pathway found for protodeboronation of **1**−**3**$_{OH}$ and *p*-anisylboronate (**10**$_{OH}$) bypasses generation of a Wheland intermediate[14e] to directly liberate the arene protodeboronation product (Ar−H). The TS for this pathway (I_B) is analogous to that previously found for the protodeboronation of 3-thienylboronate.[14m] At the TS (Figure 5), the *p*-anisyl ring is at the midpoint in its translation from the Lewis acid ($B(OH)_3$) to the Brønsted acid (OH), the process being initiated by development of a network of hydrogen bonds between incoming water and the trihydroxyboronate.

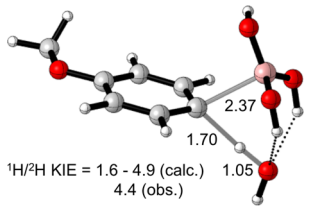

Figure 5. Transition state (M06L/6-311++G**)[32] for protodeboronation of *p*-anisylboronate (**10**$_{OH}$) via mechanism I_B (Scheme 3), where proton transfer to the ipso carbon is concerted with C−B cleavage.

A primary kinetic isotope effect (PKIE) was found to attend the rate-limiting proton transfer (Figure 5). The absolute rate differential ($k_H/k_D = 4.4$, determined in 1:1 D_2O/dioxane) was identical to the product partitioning factor (Ar−H/Ar−D = 4.4) obtained in 1:1 L_2O/dioxane (L = H/D; 50/50). The computed PKIE for the TS in Figure 5 is 1.56 (including the Wigner correction for tunneling),[35] but this is increased as explicit solvent molecules are included and becomes 2.07 when one solvating water acts as a hydrogen-bond donor to the first water molecule and 4.87 when a second solvating water is added in the same role (these are increased further when the PCM parameters for water are used). Such sensitivity to structural changes for proton-transfer KIEs was recently discussed by Aziz and Singleton.[36] Overall, we conclude that concerted mechanism I_B (Scheme 3 and Figure 5) best describes the base-catalyzed protodeboronation of electron-rich, neutral, and mildly electron-deficient arylboronic acids ($\sigma^{SL} \leq 0.7$).

6. Protodeboronation via Mechanism IV. The remaining 22 boronic acids (**7**, **9**, and **11**−**30**) are distinct from those with $\sigma^{SL} \leq 0.7$ (Figure 3), which react via pathway I_B (Scheme 3). The change in gradient ($\rho^{SL} = +3.4$) is indicative of the onset of a new process: mechanism IV. Fast-reacting 2,6-difluorophenylboronic acid (**24**, $\sigma^{SL} = 2.67$, $t_{0.5} \sim 5$ s) was selected for more detailed study. The pH−rate profile (Figure 1A) and ^{11}B NMR analysis show that mechanism IV also involves the arylboronate, **24**$_{OH}$. This species is thus a common intermediate to pathways I_B and IV, with branching dictated by aryl electron demand. The kinetics requires (pseudo) first-order branching from the arylboronate, and this essentially limits the possibilities to associative (bimolecular, H_2O, I_B), dissociative, or rearrangement (unimolecular) mechanisms.

The activation parameters for protodeboronation of **24**$_{OH}$ (determined between 22.6 and 70.4 °C using SF-ATR-FTIR; see the SI) indicate an increase in entropy at the TS ($\Delta S^{\ddagger} = +6.2$ kcal mol^{-1} K^{-1}), weighing against associative or rearrangement processes. Further studies elucidated that the stability of arylboronate **24**$_{OH}$ is mildly affected by the identity of the countercation (Figure 6). The Li^+ boronate is the most stable in the series.[37] Hydrogen-bonding interactions between water coordinated to M^+ and the triskelion hydroxyl groups of the boronate are evident in the crystal structure of [**10**$_{OH}$][$Na(H_2O)_6$] reported by Cammidge.[38] Such interactions would serve to stabilize the boronate by partial dispersion of the negative charge into the solvation sphere around the countercation.

DOI: 10.1021/jacs.7b07444
J. Am. Chem. Soc. 2017, 139, 13156−13165

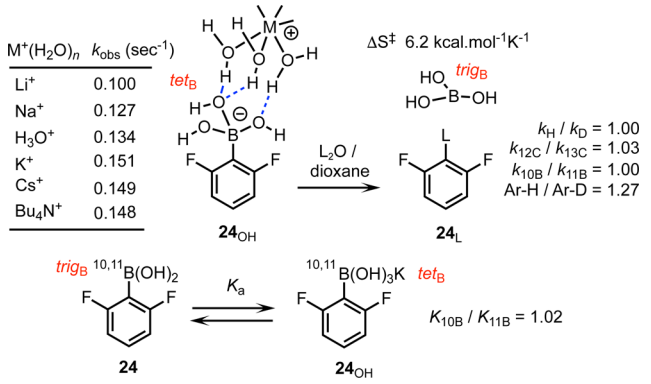

Figure 6. Protodeboronation of 2,6-difluorophenylboronate ([$\mathbf{24}_{OH}$]K^+). The kinetics for M^+ variation was determined at 70 °C, and KIEs and EIEs were determined at 27 °C by natural-abundance ^{13}C and $^{2}H/^{11}B/^{10}B$ labeling; see the SI.

In contrast to pathway I_B, the rate of protodeboronation of $\mathbf{24}_{OH}$ in 1:1 L_2O/dioxane was independent of the D/H ratio (k_H/k_D = 1.00), i.e., proton transfer is not rate-limiting. However, the product partitioning factor for $\mathbf{24}_{OH}$ is not unity (Ar−H/Ar−D = 1.26; 10 L_2O combinations; statistically corrected).[39] Elegant work by Perrin has shown that aqueous protonation of a nascent and genuinely *naked* aryl anion, generated by barrierless iodide trapping of a *p*-benzyne diradical, proceeds with a low PKIE (k_H/k_D = 1.2 ± 0.1; 55 °C) in an early transition state.[40] The partitioning factors (Ar−H/Ar−D) for protodeboronation of $\mathbf{24}_{OH}$, $\mathbf{25}_{OH}$, $\mathbf{26}_{OH}$, $\mathbf{27}_{OH}$, $\mathbf{28}_{OH}$, and $\mathbf{30}_{OH}$ in 1:1 L_2O/dioxane at 21 °C were all of a similar magnitude (average k_H/k_D = 1.26 ± 0.05).

Heavy-atom KIEs for the protodeboronation of 2,6-difluorophenylboronate ($\mathbf{24}_{OH}$) were also informative. A normal carbon PKIE (k^{12}_C/k^{13}_C = 1.03) was detected using Kwan and Jacobsen's DEPT modification of the Singleton ^{13}C NMR technique.[41] In contrast, the *net* $^{10}B/^{11}B$ KIE, estimated by double-labeling[2b] (^{2}H, ^{10}B, ^{11}B; see the SI) is unity (k^{10}_B/k^{11}_B ≈ 1.00). However, a large *inverse* KIE is known to accompany tetrahedral to trigonal reorganization at boron.[42] Indeed, a significant *equilibrium* isotope effect (EIE) (K^{10}_B/K^{11}_B = 1.02) was found for interconversion of **24** and $\mathbf{24}_{OH}$ using double-labeling[2b] in combination with Perrin's ^{19}F NMR technique.[43] This then suggests that a normal boron PKIE arising from C−B cleavage during protodeboronation of $\mathbf{24}_{OH}$ will be offset by an accompanying inverse KIE arising from tetrahedral to trigonal geometry change at boron.

Scheme 4. Substituent (X)-Controlled Branching of Base-Catalyzed Arylboronic Acid Protodeboronation via Dissociative (IV) versus Concerted (I_B) Protonolysis Mechanisms

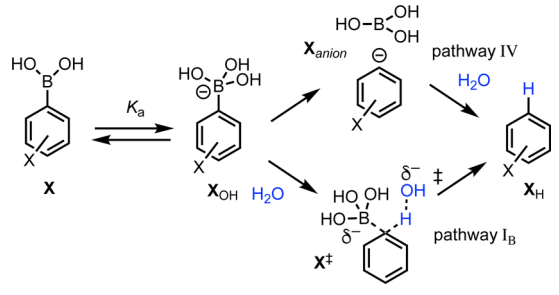

Overall then, the experimental data for protodeboronation of $\mathbf{24}_{OH}$ (Figure 6) suggest that unimolecular heterolysis of the arylboronate to generate boric acid (mechanism IV in Scheme 4) is the rate-limiting event for boronates that lie in the $\sigma_{SL} \geq 0.7$ region of Figure 3. The lowest barrier found by DFT (M06L/6-311++G**) for protodeboronation of $\mathbf{24}_{OH}$ was C−B heterolysis (Figure 7) rather than concerted proton transfer

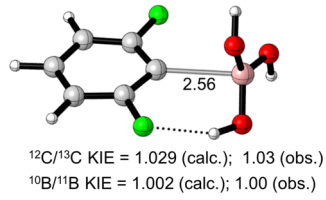

Figure 7. Transition state (M06L/6-311++G**)[32] for heterolysis of 2,6-difluorophenylboronate ($\mathbf{24}_{OH}$) via mechanism IV.

from water (mechanism I_B) ($\Delta\Delta G^{\ddagger}$ = 2.0 kcal mol^{-1}). Perrin has shown that aqueous protonation of a naked aryl anion is much faster than its combination with the counterion (i.e., M^+) to generate Ar−M.[40] Rapid protonation accounts for the absence of benzyne products when there is a nucleofuge (e.g., Br)[14j] adjacent to the boronate.[44]

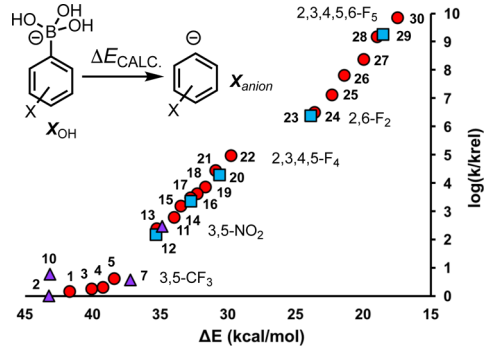

Figure 8. Rate of protodeboronation (*y* axis) as a function of electronic energy (Δ*E*) for arylboronate heterolysis to generate an aryl carbanion (*x* axis). See the SI for full details. Symbol coding: see Figure 2.

7. Analysis of Branching (I_B/IV). Two mechanisms (I_B and IV) account for the kinetics of base-catalyzed protodeboronation of all 30 arylboronic acids studied herein. The factors dictating transit via one mechanism or the other were explored computationally. The relative reaction rates for mechanism IV can be rationalized on the basis of the intrinsic energy differences (Δ*E*) calculated for the unimolecular fragmentation of the arylboronate (Figure 8).

Similar conclusions were derived from relative C−B bond orders using Wiberg bond indices[45] and from potential energy surface scans of C−B bond length (see the SI). In the latter, the stepwise increase in Δ*E* en route to the aryl anion was lower in the substrates with greatest k_{obs}. DFT transition states[32] (M06L/6-311++G**) were then calculated for mechanisms I_B and IV for all 20 isomers of $C_6H_nF_{(5-n)}B(OH)_2$ (n = 0 to 5). The activation barriers ($\Delta G^{\ddagger}$) suggest that the two mechanisms become isoenergetic at $\Delta G^{\ddagger}$ = 22.2 kcalmol^{-1} ($t_{0.5}$ ~ 12 s at 70 °C). While the analysis overestimates the σ_{SL} value (1.6) for the crossing point (Figure 9), the general trend for the transition

DOI: 10.1021/jacs.7b07444
J. Am. Chem. Soc. 2017, 139, 13156−13165

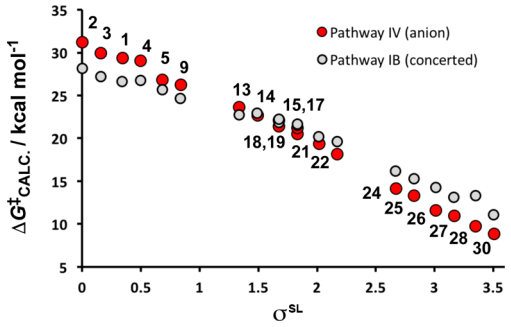

Figure 9. DFT transition state energies (M06L/6-311++G**; *y* axis) vs augmented Swain–Lupton parameter σ^{SL} (*x* axis) for all 20 isomers of $C_6H_nF_{(5-n)}B(OH)_3^-$ (n = 0 to 5) undergoing protodeboronation via pathways I_B and IV (see Scheme 4). $\sigma^{SL} = 0.69F + 0.31R + n\sigma^{o\text{-}F}$, where $\sigma^{o\text{-}F} = 1.24$ and n is the number of *o*-F substituents.

from pathway I_B to pathway IV as the net inductive effect of the substituents is raised is satisfactorily predicted.

8. Anion Stabilization through *o*-Fluoro Substitution. The above analysis provides experimental and computational evidence for a transition from mechanism I_B to mechanism IV for specific classes of substrate. Mechanism IV involves generation of a transient naked aryl anion.[46] On the basis of the differences in empirical values included in the Swain–Lupton correlations of k_{obs} (Figure 3; $\sigma^{o\text{-}F} = 1.24$) and p$K_a$ (Figure 4; $\sigma^{o\text{-}F} = 0.45$) *o*-fluoro substituents are especially efficient at facilitating *ipso*-aryl anion generation. The origins of this effect were examined through natural bond orbital (NBO) analysis[47] (M06L/6-311+G(d,p)) of the phenyl and 2,6-difluorophenyl anions ($\mathbf{2}_{anion}$ and $\mathbf{24}_{anion}$, respectively). Delocalization of negative charge into the adjacent C(2)–C(3) and C(6)–C(5) antibonding orbitals (n → σ^*) affords some stabilization of the anions. However, the major difference between the systems stems from the extent of n → σ^* delocalization into C(2)–F and C(6)–F and the accompanying increase in s character at C(1) (Figure 10). The additional stabilization energy provided by C(2,6)–F n → σ^* delocalization is around 7 kcal mol^{-1} per C–F, more than accounting for the factor of 2×10^5 difference in their rates of protodeboronation, Figure 3.

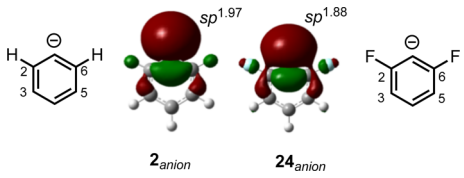

Figure 10. NLMO analyses[47b] of aryl anions $\mathbf{2}_{anion}$ and $\mathbf{24}_{anion}$ that would be generated by C–B heterolysis of boronates $\mathbf{2}_{OH}$ and $\mathbf{24}_{OH}$, respectively. See the SI for full details.

CONCLUSIONS

The mechanism of base-catalyzed protodeboronation of simple arylboronic acids, first established in 1963,[14e] has been re-examined. With the benefits of modern instrumentation (NMR, stopped-flow IR, and rapid quenched flow), the reaction kinetics has been determined at high pH, where the boronic acid is exclusively in its boronate form and the maximum rate is achieved. The study has also substantially expanded the range of arylboronic acids for which protodeboronation kinetics have been determined, including highly electron-deficient polyfluorinated systems.

Kinetic, isotopic, and computational data show that the mechanism originally proposed by Kuivila,[14e] which involves rate-limiting ipso protonation by water, is valid for the base-catalyzed protodeboronation of arylboronic acids where the combined electron demand of the substituents is below a critical point ($\sigma_{SL} \leq 0.7$; Figure 3). However, a concerted mechanism (I_B in Scheme 3) is now favored over a stepwise one (I_A).[48] Concerted proton delivery to the ipso carbon is also mediated by $ArB(OH)_2$ and $B(OH)_3$, resulting in self/autocatalysis when the pH is sufficiently close to the pK_a of the boronic acid.[14m]

When the combined electron demand of the substituents is raised above a critical point ($\sigma^{SL} \geq 0.7$; Figure 3), mechanism IV, which involves unimolecular C–B cleavage, becomes kinetically competitive over pathway I_B. This dissociative process, which formally proceeds via liberation of an aryl anion, was also considered by Kuivila[14e] but was discounted in favor of mechanism I_A on the basis of the Hammett correlation ($\rho = -2.3$) for a *m*/*p*-X-C_6H_4–$B(OH)_2$ series[23] using estimated k_{PDB} values.[49]

We have previously studied the protodeboronation of heteroaromatic systems.[14m] A key mechanistic feature in those that undergo rapid protodeboronation is a fragmentation reaction in which there is intramolecular stabilization of the departing $B(OH)_3$ during the C–B cleavage event. For the 2-pyridyl system, this stabilization is provided by hydrogen bonding with the positively charged NH (see Figure 11). However, other stabilizing interactions involving highly polarized CH and NH bonds and antibonding orbitals in the heterocycle were also found.[14m] Mechanism IV operates in a manner analogous to these processes, requiring an ability of the aryl ring to transiently accommodate the negative charge arising from fragmentation prior to rapid intermolecular protonation and, for ortho-halogenated systems, intramolecular stabilization of $B(OH)_3$ during C–B cleavage.

Perhaps surprisingly, with appropriate substituents, process IV can be significantly more effective than in even the notorious 2-pyridyl system. Consideration of all possible isomers of $C_6H_nF_{(5-n)}B(OH)_2$ exemplifies the effect: the half-lives range from 6.5 months (n = 4, meta) to 2.6 ms (n = 0), a rate differential of 6.7×10^9. Ortho-halogenated arylboronic acids undergo very fast protodeboronation[14g–k] (mechanism IV in Figure 11) predominantly because the *o*-halogen is able to accommodate an *ipso*-aryl carbanion[50] by way of n → σ^* delocalization and accompanying rehybridization with increased s character at C(1) (Figure 10). The change in mechanism from rate-limiting proton delivery (I_B) to a dissociative one means that there is no significant self/autocatalysis.[14m]

However, some additional rather subtle and more remote effects are also evident. For example, comparison of the rates of protodeboronation of **23**/**24** and **28**/**29** (Table 1) shows that *p*-MeO acts as a mild electron-donating group in **23** but as a mild electron-withdrawing group in **29**. The restriction of C_{Ar}–OMe conformations by the adjacent F substituents in **29** results in less effective conjugation of OMe to the aromatic ring compared with that in **23** and a higher field (*F*) effect. Comparison of the impact of aryl substituents on the Lewis acidity versus stability of the boronic acid (Figures 4 and 3, respectively) is also instructive. 3,5-Dinitrophenylboronic acid (**11**) is only marginally less Lewis acidic ($\Delta pK_a = 0.24$) than pentafluorophenylboronic acid (**30**)[50] but undergoes proto-

DOI: 10.1021/jacs.7b07444
J. Am. Chem. Soc. 2017, 139, 13156–13165

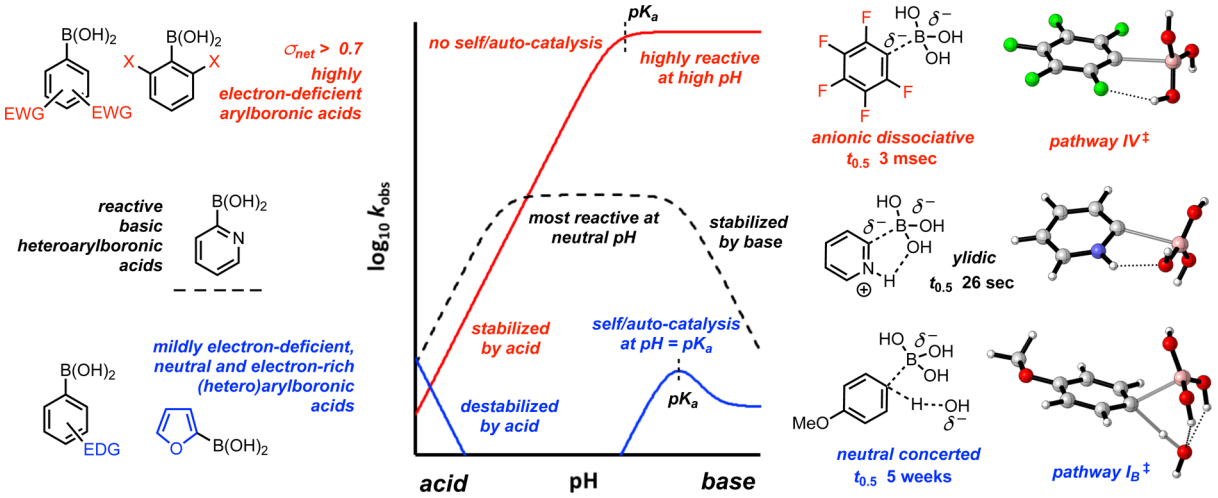

Figure 11. Pathways for arylboronic acid protodeboronation and associated effects of pH on the rate. Half-lives for reactions in 1:1 dioxane/water at 70 °C at pH > 13 (C_6H_5/C_6F_5) or at pH 7 (pyridyl) are shown. For details of self-catalysis and autocatalysis and mechanisms of protodeboronation of heteroarylboronic acids, see ref 14m.

deboronation 7 orders of magnitude more slowly. This substantial disparity arises from the differing requirements of reduced π delocalization for Lewis acidity and increased σ delocalization for protodeboronation (via mechanism IV). This is reflected in the large field (F) contribution in the Swain–Lupton analysis (Figure 3) and the differing impacts of *o*-F substitution for protodeboronation ($\sigma^{o\text{-F}} = +1.24$) versus Lewis acidity ($\sigma^{o\text{-F}} = +0.45$). The marked stability of **11** toward protodeboronation may make it of considerable use as a Lewis acid catalyst.[5] It is also worthy of note that there is no significant acid-catalyzed protodeboronation for any of the highly electron-deficient arylboronic acids studied herein. This reinforces the conclusion that reactions that can tolerate or exploit lower-pH conditions will be valuable vehicles for synthetic application of polyfluorophenyl and other highly electron-deficient arylboronic acids.[22,51]

■ ASSOCIATED CONTENT

Supporting Information

The Supporting Information is available free of charge on the ACS Publications website at DOI: 10.1021/jacs.7b07444.

Additional discussion, experimental procedures, further kinetic data and analysis, full simulation fittings, characterization data, NMR spectra, and complete ref 34 (PDF)

■ AUTHOR INFORMATION

Corresponding Author

*Guy.lloyd-jones@ed.ac.uk

ORCID

Guy C. Lloyd-Jones: 0000-0003-2128-6864

Author Contributions

⊥P.A.C. and M.R. contributed equally.

Notes

The authors declare no competing financial interest.

■ ACKNOWLEDGMENTS

The research leading to these results received funding from the European Research Council under the European Union's Seventh Framework Programme (FP7/2007–2013)/ERC Grant Agreement 340163. AstraZeneca and the EPSRC provided an iCASE Award (P.A.C.), and the Carnegie Trust provided a collaborative research grant (M.R.). We thank Dr. Ruth Dooley (Edinburgh) for assistance with pulse calibrations and acquisition of ^{13}C NMR DEPT spectra and Prof. Darren Dixon (Oxford) for discussion regarding the anomalous behavior of electron-deficient arylboronic acids.

■ REFERENCES

(1) Hall, D. G. In *Boronic Acids: Preparation and Applications in Organic Synthesis, Medicine and Materials (Volumes 1 and 2)*, 2nd ed.; Hall, D. G., Ed.; Wiley VCH: Weinheim, Germany, 2011.

(2) (a) Molander, G. A. *J. Org. Chem.* **2015**, *80*, 7837–7848. (b) Gonzalez, J. A.; Ogba, O. M.; Morehouse, G. F.; Rosson, N.; Houk, K. N.; Leach, A. G.; Cheong, P. H. Y.; Burke, M. D.; Lloyd-Jones, G. C. *Nat. Chem.* **2016**, *8*, 1067–1075. (c) Iwadate, N.; Suginome, M. J. *J. Am. Chem. Soc.* **2010**, *132*, 2548–2549.

(3) Suzuki–Miyaura coupling is the classic application. See: (a) Miyaura, N.; Yamada, K.; Suzuki, A. *Tetrahedron Lett.* **1979**, *20*, 3437–3440. For a review, see: (b) Lennox, A. J. J.; Lloyd-Jones, G. C. *Chem. Soc. Rev.* **2014**, *43*, 412–433. For selected examples of other important processes, see: Oxidative Heck reactions: (c) Cho, C. S.; Uemura, S. J. *J. Organomet. Chem.* **1994**, *465*, 85–92. Chan–Lam amination: (d) Vantourout, J. C.; Miras, H. N.; Isidro-Llobet, A.; Sproules, S.; Watson, A. J. B. J. *J. Am. Chem. Soc.* **2017**, *139*, 4769–4779. Liebeskind–Srogl coupling: (e) Liebeskind, L. S.; Srogl, J. J. *J. Am. Chem. Soc.* **2000**, *122*, 11260–11261. 1,4-Addition to enones: (f) Sakai, M.; Hayashi, H.; Miyaura, N. *Organometallics* **1997**, *16*, 4229–4231. 1,2-Addition to imines: (g) Sakai, M.; Ueda, M.; Miyaura, N. *Angew. Chem., Int. Ed.* **1998**, *37*, 3279–3281.

(4) Seiple, I. B.; Su, S.; Rodriguez, R. A.; Gianatassio, R.; Fujiwara, Y.; Sobel, A. L.; Baran, P. S. J. *J. Am. Chem. Soc.* **2010**, *132*, 13194–13196.

(5) For a review of use of arylboronic acids as catalysts, see: (a) Dimitrijević, E.; Taylor, M. S. *ACS Catal.* **2013**, *3*, 945–962. For applications, see the following lead references: In amidation reactions: (b) Ishihara, K.; Ohara, S.; Yamamoto, H. J. *J. Org. Chem.* **1996**, *61*, 4196–4197. (c) Ishihara, K.; Ohara, S.; Yamamoto, H. *Macromolecules* **2000**, *33*, 3511–3513. (d) Ishihara, K.; Ohara, S.; Yamamoto, H. *Org. Synth.* **2002**, *79*, 176–185. (e) Maki, T.; Ishihara, K.; Yamamoto, H. *Synlett* **2004**, 1355–1358. For mechanistic studies, see: (f) Al-Zoubi, R. M.; Marion, O.; Hall, D. G. *Angew. Chem., Int. Ed.* **2008**, *47*, 2876–2879. In Diels–Alder catalysis: (g) Zheng, H.; Hall, D. G. *Tetrahedron Lett.* **2010**, *51*, 3561–3564. (h) Zheng, H.; Lejkowski, M.; Hall, D. G. *Tetrahedron Lett.* **2013**, *54*, 91–94. (i) Zheng, H.; McDonald, R.; Hall, D. G. *Chem. - Eur. J.* **2010**, *16*, 5454–5460. In Friedel–Crafts

DOI: 10.1021/jacs.7b07444
J. Am. Chem. Soc. 2017, 139, 13156–13165

reactions: (j) Ricardo, C. L.; Mo, X.; McCubbin, J. A.; Hall, D. G. *Chem. - Eur. J.* **2015**, *21*, 4218−4223. (k) Liu, Y.-L.; Liu, L.; Wang, Y.-L.; Han, Y.-C.; Wang, D.; Chen, Y.-J. *Green Chem.* **2008**, *10*, 635−640. (l) Sanz, R.; Martínez, A.; Miguel, D.; Álvarez-Gutiérrez, J. M.; Rodríguez, F. *Adv. Synth. Catal.* **2006**, *348*, 1841−1845. In glycosylation reactions: (m) Nishi, N.; Nashida, J.; Kaji, E.; Takahashi, D.; Toshima, K. *Chem. Commun.* **2017**, *53*, 3018−3021. Also using borinic acids: (n) D'Angelo, K. A.; Taylor, M. S. J. *J. Am. Chem. Soc.* **2016**, *138*, 11058−11066. (o) D'Angelo, K. A.; Taylor, M. S. *Chem. Commun.* **2017**, *53*, 5978−5980. In Nazarov cyclizations: (p) Zheng, H.; Lejkowski, M.; Hall, D. G. *Tetrahedron Lett.* **2013**, *54*, 91−94. In [3 + 2] dipolar additions: (q) Zheng, H.; McDonald, R.; Hall, D. G. *Chem. - Eur. J.* **2010**, *16*, 5454−5460.

(6) Kallepalli, V. A.; Gore, K. A.; Shi, F.; Sanchez, L.; Chotana, G. A.; Miller, S. L.; Maleczka, R. E., Jr.; Smith, M. R., III *J. Org. Chem.* **2015**, *80*, 8341−8353.

(7) Ihara, H.; Suginome, M. J. *J. Am. Chem. Soc.* **2009**, *131*, 7502−7503.

(8) For example, see the following reviews: (a) Brooks, W. L. A.; Vancoillie, G.; Kabb, C. P.; Hoogenboom, R.; Sumerlin, B. S. J. *J. Polym. Sci., Part A: Polym. Chem.* **2017**, *55*, 2309−2317. (b) Vancoillie, G.; Hoogenboom, R. *Sensors* **2016**, *16*, 1736. (c) Wu, X.; Chen, X.-X.; Jiang, Y.-B. *Analyst* **2017**, *142*, 1403−1414.

(9) Vancoillie, G.; Hoogenboom, R. *Polym. Chem.* **2016**, *7*, 5484−5495.

(10) Moy, C. L.; Kaliappan, R.; McNeil, A. J. *J. Org. Chem.* **2011**, *76*, 8501−8507.

(11) Collins, J.; Nadgorny, M.; Xiao, Z.; Connal, L. A. *Macromol. Rapid Commun.* **2017**, *38*, 1600760.

(12) Jacobson, O.; Kiesewetter, D. O.; Chen, X. *Bioconjugate Chem.* **2015**, *26*, 1−18.

(13) Wang, J.; Sánchez-Roselló, M.; Aceña, J. L.; Del Pozo, C.; Sorochinsky, A. E.; Fustero, S.; Soloshonok, V. A.; Liu, H. *Chem. Rev.* **2014**, *114*, 2432−2506.

(14) (a) Ainley, A. D.; Challenger, F. *J. Chem. Soc.* **1930**, *0*, 2171−2180. (b) Kuivila, H. G.; Nahabedian, K. V. *J. Am. Chem. Soc.* **1961**, *83*, 2159−2163. (c) Kuivila, H. G.; Nahabedian, K. V. *J. Am. Chem. Soc.* **1961**, *83*, 2164−2166. (d) Nahabedian, K. V.; Kuivila, H. G. *J. Am. Chem. Soc.* **1961**, *83*, 2167−2174. (e) Kuivila, H. G.; Reuwer, J. F., Jr.; Mangravite, J. A. *Can. J. Chem.* **1963**, *41*, 3081−3090. (f) Kuivila, H. G.; Reuwer, J. F.; Mangravite, J. A. *J. Am. Chem. Soc.* **1964**, *86*, 2666−2670. (g) Frohn, H. J.; Adonin, N. Y.; Bardin, V. V.; Starichenko, V. F. *Z. Z. Anorg. Allg. Chem.* **2002**, *628*, 2834−2838. (h) Cammidge, A. N.; Crépy, K. V. L. *J. Org. Chem.* **2003**, *68*, 6832−6835. (i) Kinzel, T.; Zhang, Y.; Buchwald, S. L. *J. Am. Chem. Soc.* **2010**, *132*, 14073−14075. (j) Lozada, J.; Liu, Z.; Perrin, D. M. *J. Org. Chem.* **2014**, *79*, 5365−5368. (k) Adonin, N. Y.; Shabalin, A. Y.; Bardin, V. V. *J. Fluorine Chem.* **2014**, *168*, 111−120. (l) Noonan, G.; Leach, A. G. *Org. Biomol. Chem.* **2015**, *13*, 2555−2560. (m) Cox, P. A.; Leach, A. G.; Campbell, A. D.; Lloyd-Jones, G. C. *J. Am. Chem. Soc.* **2016**, *138*, 9145−9157.

(15) For recent examples, see: (a) Molloy, J. J.; Law, R. P.; Fyfe, J. W. B.; Seath, C. P.; Hirst, D. J.; Watson, A. J. B. *Org. Biomol. Chem.* **2015**, *13*, 3093−3102. In polymer chemistry: (b) Schroot, R.; Schubert, U. S.; Jäger, M. *Macromolecules* **2017**, *50*, 1319−1330. (c) Ji, L.; Edkins, R. M.; Sewell, L. J.; Beeby, A.; Batsanov, A. S.; Fucke, K.; Drafz, M.; Howard, J. A. K.; Moutounet, O.; Ibersiene, F.; Boucekkine, A.; Furet, E.; Liu, Z.; Halet, J.-F.; Katan, C.; Marder, T. B. *Chem. - Eur. J.* **2014**, *20*, 13618−13635.

(16) (a) Lee, C. Y.; Ahn, S. J.; Cheon, C. H. *J. Org. Chem.* **2013**, *78*, 12154−12160. (b) Ahn, S.; Lee, C. Y.; Kim, N.; Cheon, C. *J. Org. Chem.* **2014**, *79*, 7277−7285. (c) Shen, F.; Tyagarajan, S.; Perera, D.; Krska, S. W.; Maligres, P. E.; Smith, M. R., III; Maleczka, R. E. *Org. Lett.* **2016**, *18*, 1554−1557.

(17) Hansen, M. M.; Jolly, R. A.; Linder, R. J. *Org. Process Res. Dev.* **2015**, *19*, 1507−1516.

(18) For example, see: (a) Liu, C.; Li, X.; Wu, Y.; Qiu, J. *RSC Adv.* **2014**, *4*, 54307−54311. (b) Liu, C.; Li, X.; Wu, Y. *RSC Adv.* **2015**, *5*, 15354−15358. (c) Barker, G.; Webster, S.; Johnson, D. G.; Curley, R.; Andrews, M.; Young, P. C.; Macgregor, S. A.; Lee, A.-L. *J. Org. Chem.* **2015**, *80*, 9807−9816. (d) See ref 6. (e) Zhang, G.; Li, Y.; Liu, J. *RSC Adv.* **2017**, *7*, 34959−34962. (f) For early studies, see ref 14f and references therein.

(19) K_a is the equilibrium constant for aqueous interconversion of $ArB(OH)_2$ with $[ArB(OH)_3]^-$ $[H_3O]^+$; the equilibrium is pH-controlled, with the mole fractions of boronic acid (x) and boronate (x_{OH}) being given by $x_{OH} = 1/\{1 + 10^{(pK_a - pH)}\}$ and $x + x_{OH} = 1$. The hydroxide control of this equilibrium is related by the use of $K_{OH} = K_a/K_w$, where K_w is the autionization constant of water in the medium employed.

(20) Data for "Kuivila" in Scheme 1 are taken from ref 14e. These data are from reactions conducted at 90 °C in malonate-buffered water at pH 6.7 (25 °C, uncorrected). The relative rates ($k_{rel(est.)}$) were calculated by extrapolation to reactions involving 100% boronate using the pK_a values estimated by Kuivila.

(21) For a review, see: (a) Tyrrell, E.; Brookes, P. *Synthesis* **2003**, *2003*, 469−483. Also see: (b) Dick, G. R.; Woerly, E. M.; Burke, M. D. *Angew. Chem., Int. Ed.* **2012**, *51*, 2667−2672. (c) Fuller, A. A.; Hester, H. R.; Salo, E. V.; Stevens, E. P. *Tetrahedron Lett.* **2003**, *44*, 2935−2938. (d) Ishiyama, T.; Ishida, K.; Miyaura, N. *Tetrahedron* **2001**, *57*, 9813−9816. (e) Fischer, F. C.; Havinga, E. *Recl. des Trav. Chim. des Pays-Bas* **1974**, *93*, 21−24.

(22) For example, see: (a) Kohlmann, J.; Braun, T.; Laubenstein, R.; Herrmann, R. *Chem. - Eur. J.* **2017**, DOI: 10.1002/chem.201700549. (b) Korenaga, T.; Kosaki, T.; Fukumura, R.; Ema, T.; Sakai, T. *Org. Lett.* **2005**, *7*, 4915−4917. (c) Chen, L.; Sanchez, D. R.; Zhang, B.; Carrow, B. P. *J. Am. Chem. Soc.* **2017**, DOI: 10.1021/jacs.7b07687.

(23) This issue highlights the problems associated with correlations that do not include mechanistically-rich ortho substituents. For further discussion and solutions, see: Santiago, C. B.; Milo, A.; Sigman, M. S. *J. Am. Chem. Soc.* **2016**, *138*, 13424−13430.

(24) For full discussion of the mechanism of self/autocatalysis for 3-thienylboronic acid, see ref 14m.

(25) This condition assumes that $pK_{III} > pK_w$, as is found for pyrazolyl- and 3,5-dimethyl-4-isoxazolyl boronates.[14m]

(26) $B(OH)_3$ has a higher pK_a (11.03 at 70 °C) than **24** (9.15 at 70 °C), and as a result, the KOH acts catalytically when substoichiometric. Such reactions evolve from pseudo-zeroth-order to pseudo-first-order kinetics. Pure first-order kinetics is obtained with stoichiometric and excess KOH. Use of the maximum (initial) rate ($[24_{OH}]_0 \times k_{PDB}$; mM s^{-1}) allows direct comparison of all of the reactions independent of the KOH stoichiometry.

(27) Gross, K. C.; Seybold, P. G.; Peralta-Inga, Z.; Murray, J. S.; Politzer, P. J. *J. Org. Chem.* **2001**, *66*, 6919−6925.

(28) Linear regression of $\log(k_X/k_H) = \rho^{SL}(\sigma^{SL} + n\sigma^{o\text{-}F})$ or $\log(K_a^X/K_a^H) = \rho^{SL}(\sigma^{SL} + n\sigma^{o\text{-}F})$, where ρ^{SL} and $\sigma^{o\text{-}F}$ are variables and n = 0, 1, or 2 is the number of *o*-fluoro substituents.

(29) Kono, Y.; Ishihara, K.; Nagasawa, A.; Umemoto, K.; Saito, K. *Inorg. Chim. Acta* **1997**, *262*, 91−96.

(30) The rather unlikely exception to this would be if the Brønsted and Lewis acid equilibrium constants (K_a and K_{aH}) were identical in all cases.

(31) (a) Yan, J.; Springsteen, G.; Deeter, S.; Wang, B. *Tetrahedron* **2004**, *60*, 11205−11209. (b) Branch, Y. E. K.; Yabroff, D. L.; Bettman, B. *J. Am. Chem. Soc.* **1934**, *56*, 937−941.

(32) M06L/6-311++G**, incorporating solvation free energies computed as single points employing the same level of theory and the PCM formalism.[33] Solvation was incorporated using PCM settings for methanol as a solvent, which has a polarity intermediate between those of water and dioxane. This level gave the best quantitative agreement with experiment for MIDA hydrolysis.[2b] Calculations were performed using Gaussian 09[34] at 298 K and 1 atm or, for KIEs, at 343 K and 1 M.

(33) (a) Zhao, Y.; Truhlar, D. G. *Acc. Chem. Res.* **2008**, *41*, 157−167. (b) Zhao, Y.; Truhlar, D. G. *Theor. Chem. Acc.* **2008**, *120*, 215−241. (c) Tomasi, J.; Mennucci, B.; Cammi, R. *Chem. Rev.* **2005**, *105*, 2999−3094.

(34) Frisch, M. J.; et al. *Gaussian 09*, revision C.01; Gaussian, Inc.: Wallingford, CT, 2009.

DOI: 10.1021/jacs.7b07444
J. Am. Chem. Soc. 2017, 139, 13156−13165

(35) Wigner, E. *Phys. Rev.* **1932**, *40*, 749−759.
(36) Aziz, H. R.; Singleton, D. A. J. *J. Am. Chem. Soc.* **2017**, *139*, 5965−5972.
(37) For discussion and leading references on the ionic radius of the solvated hydroxonium ion, see: Iyengar, S. S.; Petersen, M. K.; Day, T. J. F.; Burnham, C. J.; Teige, V. E.; Voth, G. A. *J. Chem. Phys.* **2005**, *123*, 084309.
(38) Cammidge, A. N.; Goddard, V. H. M.; Gopee, H.; Harrison, N. L.; Hughes, D. L.; Schubert, C. J.; Sutton, B. M.; Watts, G. L.; Whitehead, A. *Org. Lett.* **2006**, *8*, 4071−4074.
(39) Control experiments/rapid pH quenching confirmed that the observed partitioning factors were not a result of, or affected by, post-protodeboronation exchange of Ar−L with L_2O/OL^-.
(40) Perrin, C. L.; Reyes-Rodríguez, G. J. *J. Am. Chem. Soc.* **2014**, *136*, 15263−15269.
(41) (a) Kwan, E. E.; Park, Y.; Besser, H. A.; Anderson, T. L.; Jacobsen, E. N. *J. Am. Chem. Soc.* **2017**, *139*, 43−46. (b) Singleton, D. A.; Thomas, A. A. *J. Am. Chem. Soc.* **1995**, *117*, 9357−9358.
(42) An analogous equilibrium isotope effect (EIE) causes isotopic fractionation of $B(OH)_3$ and $[B(OH)_4]^-$ in seawater ($K^{10}_B/K^{11}_B \geq 1.03$), making this a useful paleo-pH proxy. See: Zeebe, R. E. *Geochim. Cosmochim. Acta* **2005**, *69*, 2753−2766.
(43) (a) Perrin, C. L.; Dong, Y. J. *J. Am. Chem. Soc.* **2007**, *129*, 4490−4497.
(44) Benzynes have been generated from phenylboronates bearing *o*-nucleofuges under anhydrous conditions. For example, see: (a) Verbit, L.; Levy, J. S.; Rabitz, H.; Kwalwasser, W. *Tetrahedron Lett.* **1966**, *7*, 1053−1055. Photochemical deboronation/benzyne generation has also been reported. See: (b) Fischer, F. C.; Havinga, E. *Recl. des Trav. Chim. des Pays-Bas* **1974**, *93*, 21−24. Benzyne generation from ortho-anionic aryl triflates appears to be accelerated when arylmetalation occurs. See: (c) Dyke, A. M.; Gill, D. M.; Harvey, J. N.; Hester, A. J.; Lloyd-Jones, G. C.; Munoz, M. P.; Shepperson, I. R. *Angew. Chem., Int. Ed.* **2008**, *47*, 5067−5070.
(45) Wiberg, K. B. *Tetrahedron* **1968**, *24*, 1083−1096.
(46) For a LFER and KIE study on the generation of aryl anions by decarboxylation of arylcarboxylates, see: (a) Segura, P.; Bunnett, J. F.; Villanova, L. *J. Org. Chem.* **1985**, *50*, 1041−1045. (b) Segura, P.; Bunnett, J. F.; Villanova, L. *J. Org. Chem.* **1985**, *50*, 1041−1045. For a recent methodology involving the opposite process, reaction of an aryl anion with boron to generate an Ar−B product, see: (c) Lee, Y.; Baek, S.-y.; Park, J.; Kim, S.-T.; Tussupbayev, S.; Kim, J.; Baik, M.-H.; Cho, S. H. *J. Am. Chem. Soc.* **2017**, *139*, 976−984. We also note that exposure of pentafluorobenzene $\mathbf{30}_H$ (the product of protodeboronation of **30**) to 70 °C dioxane/L_2O at pH(D) > 13 for >100 ms results in detectable H/D exchange at C−H, presumably via $\mathbf{30}_{anion}$.
(47) (a) Reed, A. E.; Weinstock, R. B.; Weinhold, F. *J. Chem. Phys.* **1985**, *83*, 735−746. (b) Reed, A. E.; Weinhold, F. *J. Chem. Phys.* **1985**, *83*, 1736−1740.
(48) In a later work discussing the mechanism of Cd catalysis,[14f] Kuivila suggested that the correlation of the rate of base-catalyzed protodeboronation with σ, rather than σ^+, suggested an S_E2 mechanism. This change in interpretation from that originally presented[14e] appears to have been stimulated by discussion with Traylor. See: Minato, H.; Ware, J. C.; Traylor, T. G. *J. Am. Chem. Soc.* **1963**, *85*, 3024−3026.
(49) Kuivila also evaluated the impact of ortho substitution using Taft o/p rate factors. However, combinations of steric and electrostatic effects were proposed to account for the rate acceleration via pathway I_A.
(50) The rapid decompositon of $\mathbf{30}/\mathbf{30}_{OH}$ makes pK_a determination technically challenging. For example, see: Yamamoto, Y.; Matsumura, T.; Takao, N.; Yamagishi, H.; Takahashi, M.; Iwatsuki, S.; Ishihara, K. *Inorg. Chim. Acta* **2005**, *358*, 3355−3361.
(51) For examples where pentafluorophenylboronic acid (**30**) and its ester derivatives are stable under anhydrous reactions conditions, even with prolonged heating (150 °C), see: (a) Hofer, M.; Gomez-Bengoa, E.; Nevado, C. *Organometallics* **2014**, *33*, 1328−1332. (b) Hofer, M.; Genoux, A.; Kumar, R.; Nevado, C. *Angew. Chem., Int. Ed.* **2017**, *56*, 1021−1025.

DOI: 10.1021/jacs.7b07444
J. Am. Chem. Soc. 2017, 139, 13156−13165